

# Zn<sup>2+</sup>'s Ability to Alter the Distribution of Cu<sup>2+</sup> among the Available Binding Sites of A $\beta$ (1–16)-Polyethyleneglycol-ylated Peptide: Implications in Alzheimer's Disease

Chiara A. Damante,<sup>†</sup> Katalin Ösz,<sup>‡</sup> Zoltán Nagy,<sup>§</sup> Giuseppe Grasso,<sup>†</sup> Giuseppe Pappalardo,<sup>||</sup> Enrico Rizzarelli,<sup>\*,†,||</sup> and Imre Sóvágó<sup>\*,§</sup>

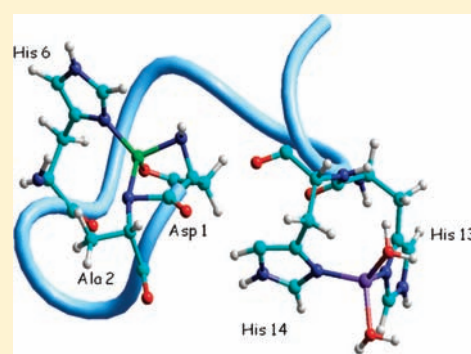
<sup>†</sup>Department of Chemical Sciences, University of Catania, V.le A. Doria 6, 95125 Catania, Italy

<sup>‡</sup>Department of Physical Chemistry, University of Debrecen, 4010 Debrecen, Hungary

<sup>§</sup>Department of Inorganic and Analytical Chemistry, University of Debrecen, 4010 Debrecen, Hungary

<sup>||</sup>CNR Institute of Biostructures and Bioimaging, V.le A. Doria 6, 95125 Catania, Italy

**ABSTRACT:** The formation of mixed copper(II) and zinc(II) complexes with A $\beta$ (1–16)-PEG has been investigated. The peptide fragment forms stable mixed metal complexes at physiological pH in which the His13/His14 dyad is the zinc(II)'s preferred binding site, while copper(II) coordination occurs at the N-terminus also involving the His6 imidazole. Copper(II) is prevented by zinc(II) excess from the binding to the two His residues, His13 and His14. As the latter binding mode has been recently invoked to explain the redox activity of the copper-A $\beta$  complex, the formation of ternary metal complexes may justify the recently proposed protective role of zinc(II) in Alzheimer's disease. Therefore, the reported results suggest that zinc(II) competes with copper for A $\beta$  binding and inhibits copper-mediated A $\beta$  redox chemistry.



## INTRODUCTION

Amyloid plaque formation in the brain plays a central role in the cognitive dysfunction characteristic of Alzheimer's disease (AD).<sup>1,2</sup> The plaques are composed primarily of 39–43 amino acid amyloid peptides (A $\beta$ ) that are derived from enzymatic cleavage of the amyloid precursor protein (APP) by  $\beta$ - and  $\gamma$ -secretases.<sup>3</sup>

Transition metals, such as Zn, Fe, and Cu, are present at elevated concentrations in AD brain deposits, suggesting that these ions may act as seeding factors,<sup>4,5</sup> while it has been proposed that A $\beta$  could have a protective role if it forms a Cu(I) complex rather than a Cu(II) complex *in vivo*.<sup>6</sup>

The oligomerization of the A $\beta$  peptides is facilitated by the presence of metal ions under physiological conditions.<sup>7–10</sup> Recently, contrasting results have been reported, as Cu(II) and Zn(II) have been indicated both as risk factors<sup>11</sup> and as protective agents in AD.<sup>12,13</sup> Inhibition of A $\beta$  aggregation<sup>14–16</sup> and formation of fibrillar or amorphous aggregates<sup>16–19</sup> caused by the peptide interaction with different metal ions have been shown to be metal concentration dependent.<sup>14</sup> TEM images showed that the aggregates are mature fibrils at low concentrations of Cu<sup>2+</sup> ions, whereas granular aggregates have been observed at high Cu<sup>2+</sup> ion concentrations.<sup>20</sup> The metal-loading of the A $\beta$  peptide involves the formation of amorphous aggregates, and a second binding site has been invoked to explain the different morphology of copper(II) complexes.<sup>19</sup> It has also been reported that neither soluble nor fibrillar forms of A $\beta$ (1–40) with Cu<sup>2+</sup> contain binuclear Cu<sup>2+</sup> sites in which two Cu<sup>2+</sup> ions are bridged by an

intervening ligand.<sup>21</sup> Moreover, other results highlight the effect of Zn<sup>2+</sup> and Cu<sup>2+</sup> on pre-existing fibrillar aggregates and are highly significant, as they provide clear evidence that the proper concentrations of different metal ions may even decrease the extent of A $\beta$  fibrillation.<sup>17</sup> Particularly, it has been suggested that (i) the misfolding mechanism is dependent on Cu<sup>2+</sup> ion concentration and (ii) the different metal complex species can lead to profound changes in A $\beta$  self-assembly kinetics, morphology, and toxicity.<sup>22</sup> Similar results have been reported on the interactions of Zn<sup>2+</sup> with A $\beta$  peptides, showing that zinc ions promote A $\beta$  aggregation.<sup>23</sup> The same study also reports that, under certain conditions, the increase of zinc(II) concentration (i) prevents fibril formation and (ii) decreases the aggregation rate. In addition, it has been found that different oligomeric species are selectively stabilized by the changes of Zn<sup>2+</sup> concentrations and that Zn<sup>2+</sup> ions possibly promote interpeptide aggregation modes.<sup>24</sup> This complexity rendered by zinc(II) coordination has been invoked to explain zinc selectivity in precipitating aggregation intermediates.<sup>23</sup> In summary, different morphologies and related toxicities<sup>22</sup> have been attributed to different coordination modes experienced by copper(II) and zinc(II),<sup>25,26</sup> and many studies have been performed to clarify the major metal binding sites of A $\beta$  peptides.<sup>27–29</sup> However, the literature has not achieved consensus as to the stoichiometry and binding affinity

Received: May 24, 2010

Published: May 25, 2011

of A $\beta$  with metals such as copper(II) and zinc(II). For example, the estimated values for the binding constants reported in the literature in the case of Cu(II)-A $\beta$  range from  $4.0 \times 10^5 \text{ M}^{-1}$  to  $1.5 \times 10^{11} \text{ M}^{-1}$ .<sup>30,31</sup> The latter Cu<sup>2+</sup> ion affinity for A $\beta$  supports a modified amyloid cascade hypothesis in which Cu<sup>2+</sup> is central to A $\beta$  neurotoxicity.<sup>31</sup> Nevertheless, there is general agreement that, in the A $\beta$  peptide, the metal binding sites are located at the N-terminal hydrophilic region encompassing the amino acid residues 1–16, whereas the C-terminal region, which contains hydrophobic amino acid residues, is not believed to be associated with any direct interaction with metal ions. Although it is already reported that amyloid- $\beta$  can host more than one copper(II)<sup>32–34</sup> or zinc(II)<sup>33,35</sup> ion per peptide molecule and many studies have already described the stoichiometry of metal-A $\beta$  peptide complexes,<sup>33,36</sup> the precipitate formation from metal-A $\beta$  peptide solutions did not allow the complete characterization of the solution equilibria and the structural properties of these polynuclear systems.

It is known that the conjugation with the polyethylene glycol (PEG) moiety enhances the water solubility of hydrophobic peptides. Thus, the conjugation of the A $\beta$ (1–16) peptide sequence with a PEG moiety allowed us to study the stoichiometry, the speciation, the affinity, and the co-ordination features of the copper(II),<sup>26</sup> zinc(II),<sup>25</sup> and nickel(II)<sup>37</sup> simple complexes formed with a peptide ligand encompassing the 1–16 amino acid sequence of A $\beta$  even at high metal to ligand ratios in aqueous solution. It was demonstrated that: (i) the A $\beta$ (1–16)PEG ligand can accommodate up to three or four Zn<sup>2+</sup> or Cu<sup>2+</sup> ions, respectively; (ii) at a low M<sup>2+</sup>/A $\beta$  ratio, the M<sup>2+</sup> is coordinated to the histidines of the A $\beta$  peptide, giving rise to macrochelate rings, while, as the M<sup>2+</sup>/A $\beta$  ratio increases, more than one complex species forms with different coordination modes due to the metal-assisted deprotonation of the amide nitrogens; (iii) the two metal ions prefer occupying different metal binding sites in the mononuclear species in the physiological pH range: the N-terminal amino group represents the primary anchor site for Cu<sup>2+</sup>, while the His13 and His14 residues are the prevailing chelating ligands for Zn<sup>2+</sup>.<sup>25,26</sup> The different coordination modes observed by changing the metal to A $\beta$ -peptide ratios recall the different aggregation morphologies previously mentioned<sup>17</sup> and might have significant biological consequences in terms of A $\beta$  fibril formation and toxicity. On the other hand, the differences in the coordination behavior of the two metal ions prompted us to study the formation, the affinity, and the binding features of mixed copper(II) and zinc(II) complexes with A $\beta$ (1–16)-PEG.

Different experimental techniques were used to study the ternary copper(II)–zinc(II)–A $\beta$ (1–16)-PEG complex. In addition to potentiometric measurements, which provided us with the formation constant values and the speciation of mixed metal complexes, UV–vis, CD, and EPR spectroscopic investigations were carried out to ascertain the ability of zinc(II) to perturb the copper(II) binding modes previously observed in simple complex species.<sup>26</sup>

Since a direct evaluation of the potentiometric and spectroscopic data in the full-length A $\beta$ (1–16)PEG would be hindered by the presence of several potentially copper(II) and zinc(II) binders (represented by the His6, His13, His14, Asp1, Asp7, Glu3, Glu11, and Tyr10 side chains in addition to the N-terminal amino group), two shorter A $\beta$  peptide fragments, namely, A $\beta$ (1–6) and AcA $\beta$ (8–16)Y10A, each one containing a potential copper(II) or zinc(II) binding site, were comparatively



**Figure 1.** Amino acid sequences of the peptide fragments of the amyloid- $\beta$  peptide. Black and gray arrows indicate trypsin and elastase cleavage sites, respectively.

studied to assess the involvement of the different amino acid residues in the binding to metal ions within the whole A $\beta$  peptide.

In addition, limited proteolysis experiments together with mass spectrometry analysis of the peptide mixture were carried out in order to give further evidence of the coordination features for both binary and ternary metal–A $\beta$  complexes. The potential implications of different metal complexes and of their coordination features are discussed, and a justification of the protective role of zinc in comparison with copper is proposed.

## MATERIALS AND METHODS

**Peptide Synthesis and Purification.** The amino acid sequences of the three A $\beta$  peptides used in this study are reported in Figure 1, while their synthesis has been described elsewhere.<sup>26</sup>

**Potentiometric and Spectroscopic Measurements.** The potentiometric titrations were performed with 3 cm<sup>3</sup> samples, exploring the concentration range of  $1 \times 10^{-3}$  to  $3 \times 10^{-3} \text{ mol dm}^{-3}$  with a metal ion-to-ligand ratio of 1:1:1 in the case of the AcA $\beta$ (8–16)Y10A (referred to as L), whereas for A $\beta$ (1–16)PEG (indicated as L'), ratios of 1:1:1, 2:1:1, and 1:2:1 Cu(II)/Zn(II)/L' were studied. All measurements were carried out at 298 K and at a constant ionic strength of 0.2 mol dm<sup>−3</sup> KCl. pH measurements were made with a MOLSPIN pH-meter equipped with a 6.0234.100 combined electrode (Metrohm) and a MOL-ACS microburet controlled by a computer. Formation constants (log  $\beta_{opqr}$ ) were calculated by means of the computational programs PSEQUAD,<sup>38</sup> SUPERQUAD,<sup>39</sup> and HYPERQUAD<sup>40</sup> by using eqs 1 and 2 (in the case of A $\beta$ (1–16)PEG, L is replaced by L').

$$oM + pM' + qH + rL = M_oM'_pH_qL_r \quad (1)$$

$$\beta_{opqr} = [M_oM'_pH_qL_r] / [M]^o [M']^p [H]^q [L]^r \quad (2)$$

The coefficients  $o$ ,  $p$ ,  $q$ , and  $r$  are integers and, for example, in the case of simple metal binding associated with deprotonation, they can have negative values. The number of experimental data (cm<sup>3</sup> – pH) was around 150 to 200 and 250 to 300 for each titration curve recorded in the mixed metal systems of L and L', respectively. These numbers are 1 or 2 orders of magnitude higher than the numbers of the unknown constants of mixed metal species (4 and 23 for L and L', respectively). Taking into account the experimental errors of the volume of titrant ( $\Delta v = 0.001 \text{ cm}^3$ ) and pH values ( $\Delta \text{pH} = 0.002$ ) the  $\sigma$  values<sup>38</sup> varied in the range of 0.08 to 0.2, indicating a good fit of the experimental and calculated titration curves.

UV–vis spectra of complexes were recorded on a Hewlett-Packard HP 8453 diode array spectrophotometer in the same concentration range as used for potentiometric measurements. All of the CD measurements were carried out at 25 °C under a flow of nitrogen on a JASCO

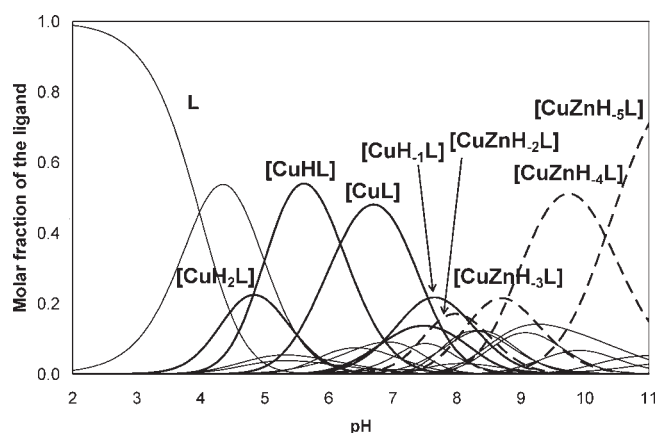


**Figure 2.** Species distribution diagram of the copper(II) and zinc(II) mixed complexes with AcA $\beta$ (8–16)Y10A (L) ( $c_{\text{Zn(II)}} = c_{\text{Cu(II)}} = c_{\text{L}} = 2 \times 10^{-3} \text{ mol dm}^{-3}$ ).

model J-810 spectropolarimeter. A Bruker Elexsys E500 CW-EPR spectrometer driven by a PC running the xEpr program under Linux and equipped with a Super-X microwave bridge operating at 9.3–9.5 GHz and a SHQE cavity was used throughout this work. All EPR spectra of frozen solutions of copper(II) complexes were recorded at 150 K by means of a variable-temperature apparatus. The EPR parameters were obtained directly from the experimental spectra obtained at the maximum concentration of the particular species for which well resolved separations were observed. Other details are as previously reported.<sup>25,26</sup>

#### Limited Proteolysis Experiments and LC-ESI-MS Analysis.

Limited proteolysis experiments were carried out by incubating soluble A $\beta$ (1–16)PEG (peptide concentration =  $1 \times 10^{-4} \text{ mol dm}^{-3}$ ) with trypsin using an enzyme to substrate ratio of 20:1 (w/w). The metal complex solutions were prepared by dissolving the peptide and ZnSO<sub>4</sub> or CuSO<sub>4</sub> at metal ion to ligand ratios between 3:1 and 1:1 for zinc(II) and between 4:1 and 1:1 for copper(II). Trypsin digestion experiments were all performed in an ammonium bicarbonate buffer (pH 8.0) at 37 °C for 30 min in a monomode microwave reactor (CEM Focused Microwave Synthesis, Model Discover, CEM Co.) at 6 W. The actual temperatures of reaction solutions were measured with a thermocouple after microwave irradiation. The microwave was turned on for 30 min. After digestion, the vials were removed from the reactor and prepared for further HPLC and ESI-MS analysis.

In the case of peptide hydrolysis by leukocyte elastase, the peptide was dissolved in ammonium bicarbonate (pH 8.0) to a concentration of  $1 \times 10^{-4} \text{ mol dm}^{-3}$ , either in the absence or in the presence of copper(II) and zinc(II). Metal to peptide ratios between 3:1–1:1 and 4:1–1:1 were used for zinc(II) and copper(II), respectively. Samples were incubated with elastase by using an enzyme to substrate ratio of 20:1 (w/w). Elastase digestion experiments were all performed at 37 °C for 75 min in a monomode microwave reactor at 6 W. After digestion, the vials were removed from the reactor and prepared for further HPLC and ESI-MS analysis.

After proteolysis with trypsin or elastase, peptide digests were separated using a LCQ-DECA XP ion trap Finnigan instrument using an electrospray ionization (ESI) interface and equipped with Thermo photodiode array detector with detection at 222 nm. Samples were analyzed eluting with solvents A (0.05% TFA in water) and B (0.05% TFA in acetonitrile) on a BioBasic C<sub>18</sub> 50  $\times$  2.1 mm (300 Å pore size, 5  $\mu\text{m}$  particle size) column, at flow rate of 250  $\mu\text{L}/\text{min}$ . The temperature was controlled at 25 °C. Samples were injected into the column equilibrated to 100% solvent A and eluted with a linear gradient of 0%–25% solvent B over a 15 min period. The separation was monitored by absorbance at 222 nm and by ESI-MS. Eluted peptides were detected

**Table 1.** Formation Constants ( $\log \beta_{\text{opqr}}$ ) of the Mixed Metal Complexes of Copper(II) and Zinc(II) with AcA $\beta$ -(8–16)Y10A (L) (Standard Deviations in Parentheses,  $T = 298 \text{ K}$ ,  $I = 0.2 \text{ mol dm}^{-3} \text{ KCl}$ )

species	$\log \beta$	pK	amide deprotonation
[CuZnH <sub>2</sub> L]	−2.54(3)		
[CuZnH <sub>3</sub> L]	−10.77(3)	8.23	−2 m/−3 m
[CuZnH <sub>4</sub> L]	−19.56(8)	8.79	−3 m/−4 m
[CuZnH <sub>5</sub> L]	−29.88(10)	10.32	−4 m/−5 m

in a completely automated fashion via 100  $\mu\text{m}$  i.d. fused silica. The spectra were acquired in the positive ion mode, and the instrumental conditions were as follows: needle voltage, 3.0 kV; flow rate, 3–5  $\mu\text{L}/\text{min}$ ; source temperature, 250–300 °C;  $m/z$  range, 50–4000; cone potential, 37 V; tube lens offset, −60 V.

## RESULTS AND DISCUSSION

**Affinity, Binding Sites, and Coordination Modes of Ternary Cu<sup>2+</sup>–Zn<sup>2+</sup>–A $\beta$  Peptides Complexes by Potentiometric and Spectroscopic Investigations.** We started our systematic study of the metal ion interaction with A $\beta$  peptide fragments from the A $\beta$ (1–6) peptide that potentially contains two binding sites for metal ion coordination, namely, the N-terminal amino and the His6 imidazole. We previously found that unlike copper(II), which gives both mono- and multiple-nuclear species with the A $\beta$ (1–6) peptide,<sup>26</sup> zinc(II) can form only mononuclear complexes with this peptide ligand.<sup>25</sup> It is therefore not surprising that in the presence of both copper(II) and zinc(II) we have not observed any formation of mixed metal complexes with the A $\beta$ (1–6) peptide in the pH range investigated. On the contrary, the C-terminal region of the A $\beta$ (1–16) peptide, namely, AcA $\beta$ -(8–16)Y10A, can form multinuclear mixed metal complexes, as previously found for copper(II) or zinc(II) binary complexes (see Figure 2).<sup>25,26</sup> The formation constants (see Table 1) refer to a copper(II)–zinc(II)–AcA $\beta$ (8–16)Y10A 1:1:1 system (the substitution of the tyrosine with the alanine residue does not affect the potentiometric results, as previously shown for the simple metal complexes).<sup>25,26</sup>

The speciation shows that the complex formation starts at pH > 3.0 with the formation of only copper(II) mononuclear species. At this stage, the zinc(II) is predominately in an uncomplexed form. In the mononuclear species, the copper(II) is coordinated *via* the two imidazole rings of the histidyl residues, in the form of a macrochelate, as it was previously reported for the copper(II) complexes formed at a 1:1 metal to ligand ratio.<sup>26</sup> This conclusion is definitely supported on the basis of the spectroscopic data, since the CD and UV–vis (see Figures 3 and 4) recorded on the mixed metal system at low pH values are identical to those previously reported for the copper(II)–AcA $\beta$ (8–16)Y10A 1:1 system.<sup>26</sup> The formation of the ternary metal complexes occurs above pH 7.0, in parallel with the deprotonation of the amide nitrogens (see Figure 2). The inspection of the pK values pertinent to amide deprotonations (see Table 1) indicates that only the last deprotonation step involves the lysine residue, and the UV–vis and CD spectra of mixed metal complexes (see Figures 3 and 4) are comparable to those obtained for the binary copper(II) complex species.<sup>26</sup> Taken together, these results indicate that the coordination mode of the copper(II) is not modified by the additional zinc(II) binding. In other words, zinc(II) is not able to replace the



copper(II) from its favored metal binding site and is forced to interact only with the free sites. At basic pH values, the copper(II) has been shown to preferentially coordinate via the His13 and an increasing number of amide nitrogens which are deprotonated toward the N-terminal side.<sup>26</sup> Again, the comparison of the spectroscopic data (i.e., the CD and UV-vis spectra recorded

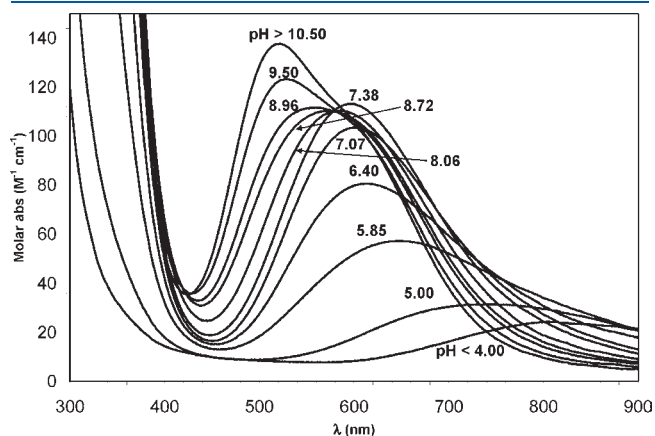


**Figure 3.** UV-vis absorption spectra of the copper(II) and zinc(II) mixed complexes with AcAβ(8-16)Y10A as a function of pH ( $c_{\text{Zn(II)}} = c_{\text{Cu(II)}} = c_{\text{L}} = 0.80 \times 10^{-3} \text{ mol dm}^{-3}$ ).

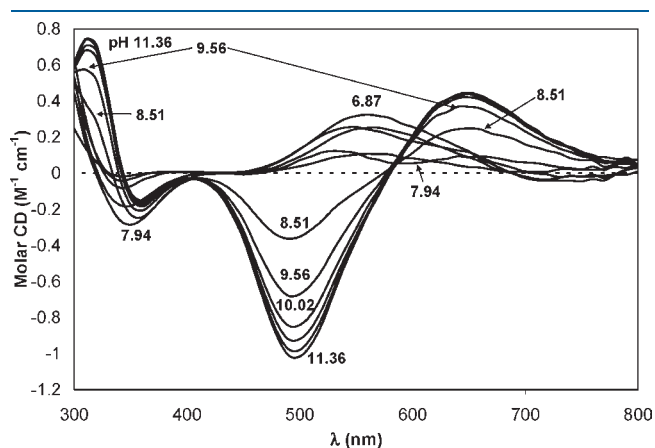


**Figure 4.** CD spectra of the copper(II) and zinc(II) mixed complexes with AcAβ(8-16)Y10A as a function of pH ( $c_{\text{Zn(II)}} = c_{\text{Cu(II)}} = c_{\text{L}} = 0.80 \times 10^{-3} \text{ mol dm}^{-3}$ ).

for the 1:1 copper(II)–AcAβ(8-16)Y10A system<sup>26</sup>) proves unambiguously that an identical coordination mode of the copper(II) is conserved also in the mixed metal complexes (see Figures 3 and 4). As a consequence, the zinc(II) should be coordinated *via* the imidazole ring of His14 and one or two deprotonated amide nitrogens toward the C-terminal side of this histidine as observed for the zinc(II)–AcAβ(8-16)Y10A 2:1 system.<sup>25</sup>

Our previous studies have unambiguously proved the formation of mono-, di-, and trinuclear complexes in the zinc(II)–Aβ(1-16)PEG system.<sup>25</sup> Moreover, the same experimental approach demonstrated that, in the presence of an excess of copper(II), Aβ(1-16)PEG can host even four equivalents of copper(II) per peptide molecule.<sup>26</sup> These observations, together with those reported above for the mixed metal complexes of AcAβ(8-16)Y10A, suggest that also Aβ(1-16)PEG, in the presence of copper(II) and zinc(II) ions, may bind both metal ions in the form of mixed metal zinc(II)–copper(II) complexes. Therefore, potentiometric and spectroscopic measurements have been performed at three different metal ion to peptide ligand (referred to as L') ratios, namely, Cu(II)/Zn(II)/L' = 1:1:1, 2:1:1, and 1:2:1 ratios. The computer evaluation of the potentiometric data reveals that all major stoichiometries, comprising binuclear and trinuclear species, are present in solution in different protonation stages. The general formulas of the mixed

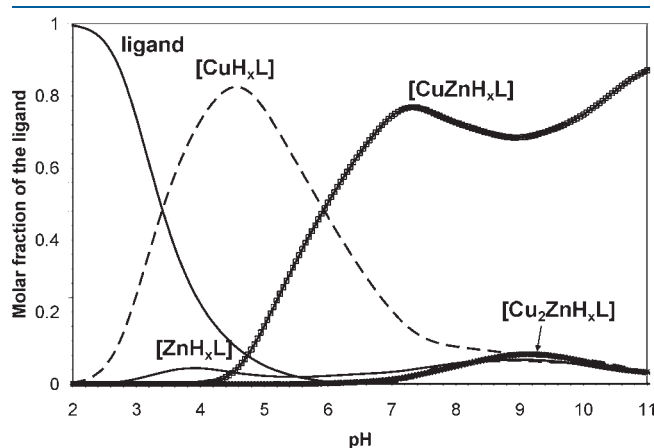


**Figure 5.** Species distribution diagram of the complexes formed in the zinc(II)–copper(II)–Aβ(1-16)PEG system ( $c_{\text{Zn(II)}} = c_{\text{Cu(II)}} = c_{\text{L}} = 2 \times 10^{-3} \text{ mol dm}^{-3}$ ).

**Table 2.** Formation Constants ( $\log \beta_{\text{opqr}}$ ) of the Mixed Metal Complex Species of Copper(II) and Zinc(II) with Aβ(1-16)PEG (L') (Standard Deviations in Parentheses,  $T = 298 \text{ K}$ ,  $I = 0.2 \text{ mol dm}^{-3} \text{ KCl}$ )

dinuclear $\text{CuZnH}_q\text{L}'$ complexes		trinuclear $\text{Cu}_2\text{ZnH}_q\text{L}'$ complexes		trinuclear $\text{CuZn}_2\text{H}_q\text{L}'$ complexes	
species	$\log \beta_{11q1}$	species	$\log \beta_{21q1}$	species	$\log \beta_{12q1}$
$\text{CuZnH}_3\text{L}'$	39.67(9)	$\text{Cu}_2\text{ZnL}'$	25.95(10)	$\text{CuZn}_2\text{H}_{-2}\text{L}'$	8.45(9)
$\text{CuZnH}_2\text{L}'$	34.16(4)	$\text{Cu}_2\text{ZnH}_{-1}\text{L}'$	18.63(10)	$\text{CuZn}_2\text{H}_{-3}\text{L}'$	0.22(9)
$\text{CuZnHL}'$	27.71(4)	$\text{Cu}_2\text{ZnH}_{-2}\text{L}'$	11.98(10)	$\text{CuZn}_2\text{H}_{-4}\text{L}'$	−8.39(9)
$\text{CuZnL}'$	20.40(6)	$\text{Cu}_2\text{ZnH}_{-3}\text{L}'$	4.47(9)	$\text{CuZn}_2\text{H}_{-5}\text{L}'$	−18.07(10)
$\text{CuZnH}_{-1}\text{L}'$	12.63(7)	$\text{Cu}_2\text{ZnH}_{-4}\text{L}'$	−3.23(7)	$\text{CuZn}_2\text{H}_{-6}\text{L}'$	−27.78(8)
$\text{CuZnH}_{-2}\text{L}'$	3.93(9)	$\text{Cu}_2\text{ZnH}_{-5}\text{L}'$	−12.04(7)		
$\text{CuZnH}_{-3}\text{L}'$	−5.16(8)	$\text{Cu}_2\text{ZnH}_{-6}\text{L}'$	−21.48(7)		
$\text{CuZnH}_{-4}\text{L}'$	−15.03(9)	$\text{Cu}_2\text{ZnH}_{-7}\text{L}'$	−31.78(8)		
$\text{CuZnH}_{-5}\text{L}'$	−25.32(6)	$\text{Cu}_2\text{ZnH}_{-8}\text{L}'$	−42.86(9)		

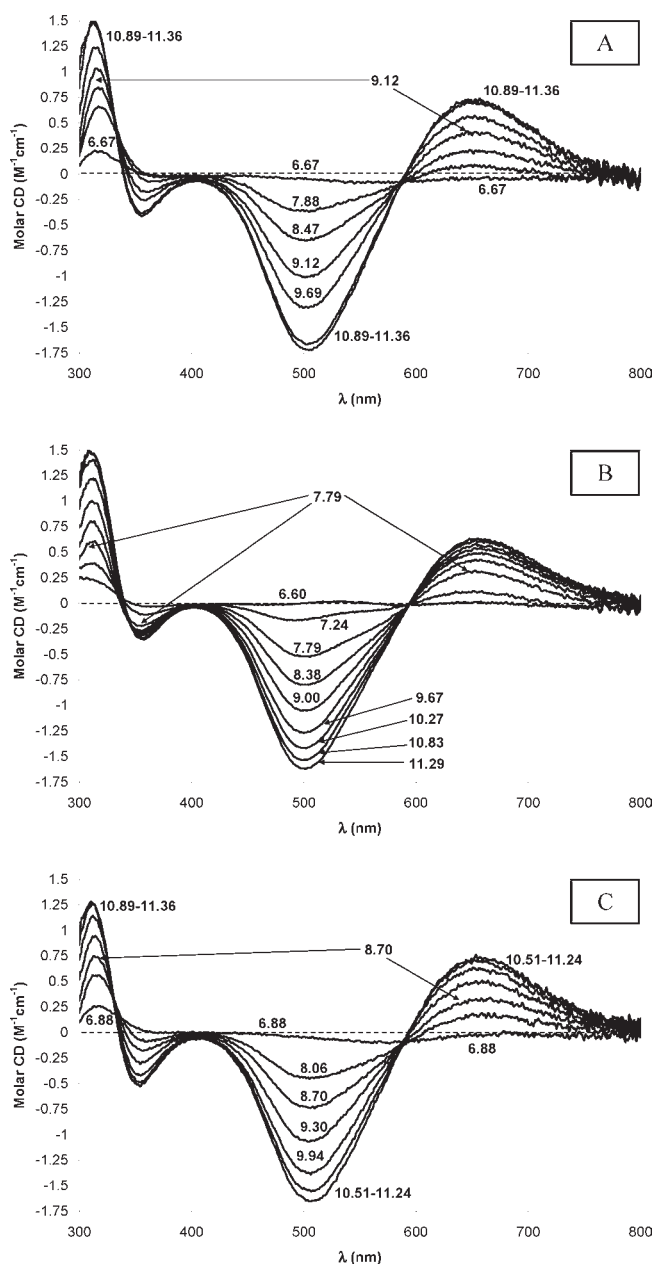


**Figure 6.** CD spectra of the copper(II) and zinc(II) mixed complexes with  $A\beta(1-16)PEG$  as a function of pH and at different metal to ligand ratios: (A)  $L'/Cu(II)/Zn(II)$  1:1:1; (B)  $L'/Cu(II)/Zn(II)$  1:2:1; (C)  $L'/Cu(II)/Zn(II)$  1:1:2 ( $c_{L'} = 0.80 \times 10^{-3} \text{ mol dm}^{-3}$ ).

metal species can be given as  $[CuZnH_qL']$ ,  $[Cu_2ZnH_qL']$ , and  $[CuZn_2H_qL']$ . The formation constants of these complexes are listed in Table 2. Figure 5 shows the overall concentrations of these species plotted as a function of the pH. Yet, the total number of individual species is very high in such a system, because all of the binary copper(II) and zinc(II) complexes and the ternary mixed metal species can exist in the solution. Therefore, the  $[CuH_xL']$ ,  $[ZnH_xL']$ ,  $[CuZnH_xL']$ , and  $[Cu_2ZnH_xL']$  species, reported in the diagram obtained at a 1:1:1  $Cu(II)/Zn(II)/L'$  ratio, represent the sum of the differently protonated binary and ternary complex species. It is clear from Figure 5 that the peptide ligand is totally bound to the metal(s) above a pH of 6.0. Binary copper(II) complexes are present in the acidic pH

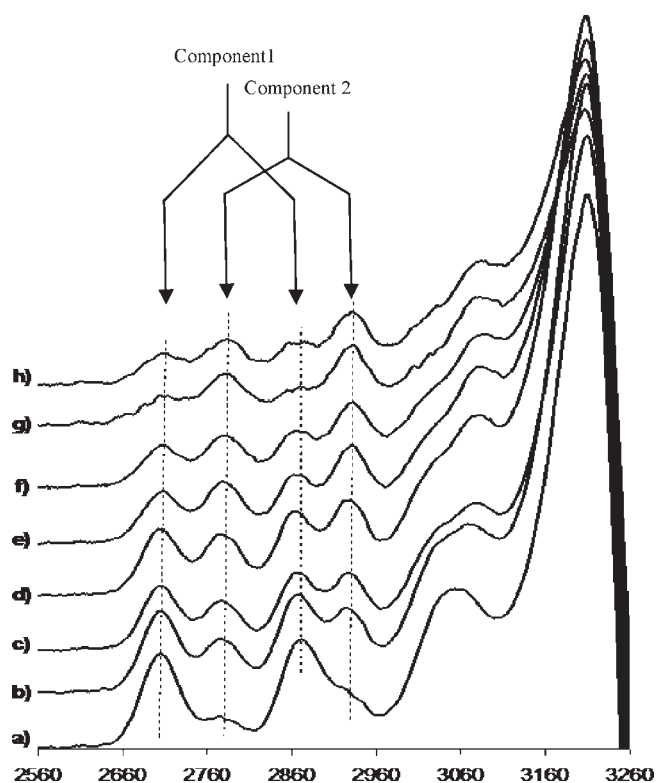


**Figure 7.** EPR spectra of  $Cu/A\beta(1-16)PEG$  solutions obtained by adding increasing amounts of zinc(II) ions to a solution containing copper(II):  $A\beta(1-16)PEG$  in 1:1 metal to peptide ratio at pH 7.0,  $[L'] = 1.4 \times 10^{-3} \text{ mol dm}^{-3}$ . (a)  $L'/Cu(II)/Zn(II)$  1:1:0; (b)  $L'/Cu(II)/Zn(II)$  1:1:1; (c)  $L'/Cu(II)/Zn(II)$  1:1:1.2; (d)  $L'/Cu(II)/Zn(II)$  1:1:1.5; (e)  $L'/Cu(II)/Zn(II)$  1:1:2; (f)  $L'/Cu(II)/Zn(II)$  1:1:2.5; (g)  $L'/Cu(II)/Zn(II)$  1:1:3; (h)  $L'/Cu(II)/Zn(II)$  1:1:4.

range (the concentration of the binary zinc(II) complexes is negligible), while the 1:1:1 mixed metal species are the prevailing complexes at a pH of 7.0. In the case of the 1:2:1  $Cu(II)/Zn(II)/L'$  ratio, the excess of zinc(II) ions is bound in the neutral and slightly basic pH range ( $[CuZn_2H_xL']$  species), where the metal ion coordination through the deprotonated amide nitrogen is favored (data not shown).

CD experiments in the visible wavelength region were carried out to assess whether the presence of zinc can alter the coordination modes of the copper ion observed previously in the binary complexes.<sup>23</sup> The CD measurements on the copper(II) and zinc(II) mixed complexes with  $AcA\beta(1-16)PEG$  were recorded as a function of pH. The CD curves reported in Figure 6 were obtained at the same metal to ligand ratios used to run the potentiometric measurements (i.e.,  $Cu(II)/Zn(II)/AcA\beta(1-16)PEG$  1:1:1, 2:1:1, 1:2:1). The CD profiles observed in the mixed metal system are not dissimilar from those reported for the simple copper(II) complexes with  $AcA\beta(1-16)PEG$ .<sup>26</sup> Only slight differences are seen at 350 nm, in the region where optically active ligand to metal charge–transfer transition (LMCT) normally occurs.<sup>41,42</sup> This may reflect subtle changes in the disposition of the coordinated imidazole side chains around the copper(II), although a reorganization of the number of imidazole side chains within the copper(II) binding sites, as a consequence of the competition of the zinc(II), cannot be ruled out. On the whole, considering that the induced dichroic bands observed in these spectra come exclusively from the copper(II) ions, the almost unaltered CD pattern suggests that, at least at these molar

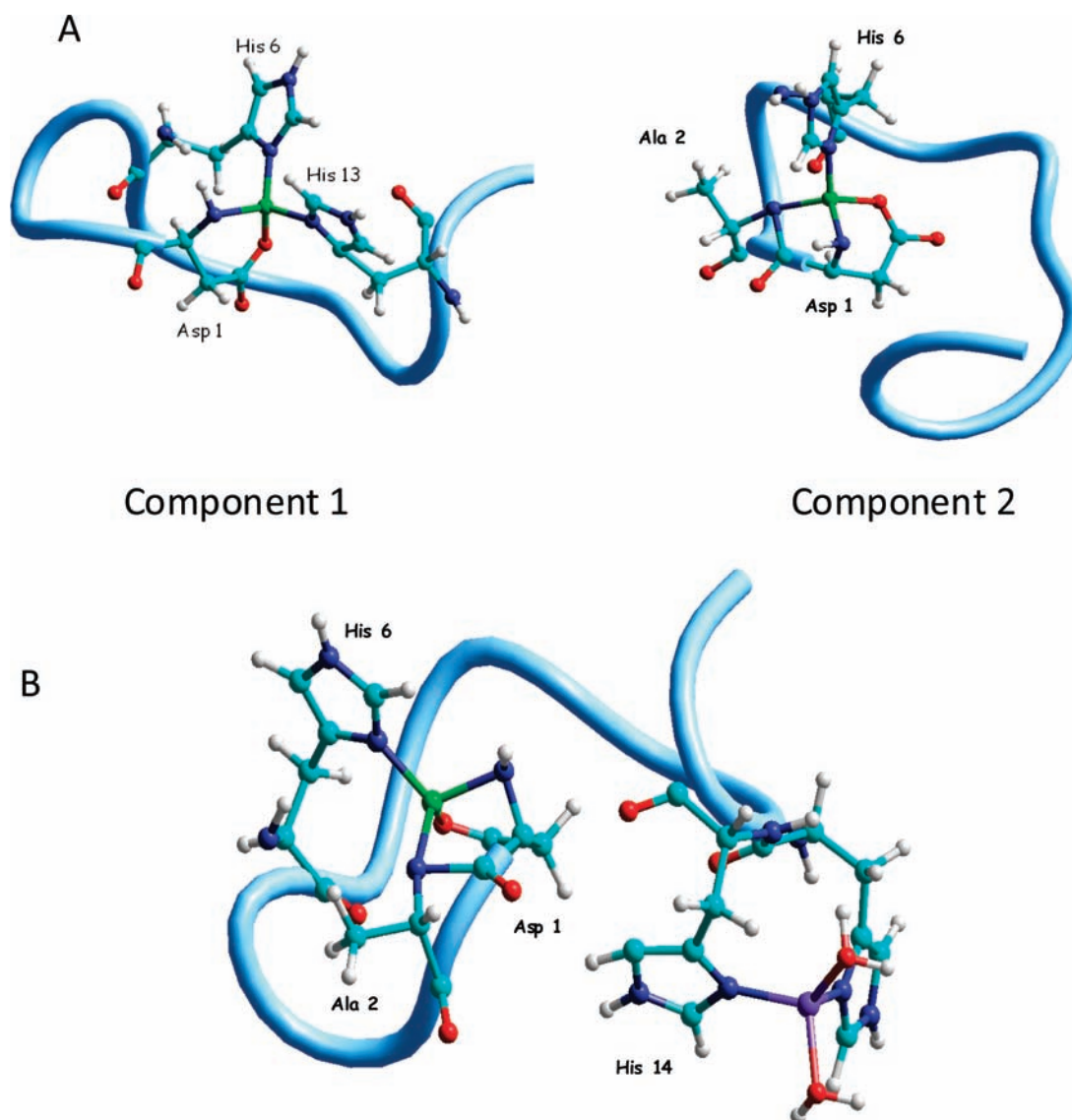


**Figure 8.** (A) Proposed structures of components 1 and 2 of the copper(II) complexes. (B) Proposed structure of the mixed metal complex. Only amino acid residues involved in metal complexation are shown for clarity.

ratios, zinc coordination does not totally replace copper(II) from its preferred binding sites in the peptide sequence. To further inquire into the ability of zinc ions to modify copper(II) distribution along the  $A\beta(1-16)$  sequence, we employed a direct competition between copper and zinc to characterize the binding sites in the  $A\beta$  N-terminus peptide fragment derivative, with the copper(II) binding monitored by X-band EPR (Figure 7). We have recently shown that two copper(II) complexes with the  $A\beta(1-16)$  PEG peptide coexist at a 1:1 metal to ligand ratio in the 6.7–7.9 pH range.<sup>26</sup> The major species observed at a pH of 7.0 was characterized by the following magnetic parameters:  $g_{II} = 2.265(1)$  and  $A_{II} = 175(1) \times 10^{-4} \text{ cm}^{-1}$  (coinciding with component 1 in Figure 7). These values can be assigned to a complex species in which the copper(II) is bound to the N-terminal amino and aspartyl carboxylate groups, in a six-member chelate ring, while two additional  $N_{im}$  donors complete the metal's coordination sphere (see Figure 8A, component 1).<sup>26</sup> A further increase of the pH led to the formation of another species (see Figure 8A, component 2) in which the copper(II) was coordinated in a

$(NH_2, N^-)$  five-membered chelate ring, stabilized by the macrochelation with one  $N_{im}$  donor. This hypothesis was supported by the  $g_{II}$  and  $A_{II}$  values measured for this species ( $g_{II} = 2.236(1)$ ,  $A_{II} = 151(1) \times 10^{-4} \text{ cm}^{-1}$ ), whose magnetic parameters were similar to those reported for 3N complex species present at physiological pH in the Cu– $A\beta(1-6)$  system.<sup>26</sup> The examination of EPR band profiles shown in Figure 7 indicates that, at a pH of 7.0, the growth of a second set of signals is a function of the increasing zinc(II) concentration. This suggests that copper(II) binding mode shifts mostly from component 1, in the absence of zinc(II), to a major species represented by component 2 ( $Zn^{2+}$  is diamagnetic and therefore has no EPR signal.). The magnetic parameters, measured directly from the experimental EPR spectrum recorded in the presence of a 4-fold molar excess of zinc(II) with respect to both the  $L'$  ligand and Cu(II), are  $g_{II} = 2.273(1)$  and  $A_{II} = 170(2) \times 10^{-4} \text{ cm}^{-1}$  and  $g_{II} = 2.228(1)$  and  $A_{II} = 157(1) \times 10^{-4} \text{ cm}^{-1}$ , respectively, for components 1 and 2. Interestingly, the magnetic parameters of component 2 are again very similar to those obtained for the  $[CuH_{-1}L]$  complex species of the

**Table 3. Peptide Fragments Detected by ESI-MS after Trypsin or Elastase Digestion of A $\beta$ (1-16)PEG Peptide<sup>a</sup>**

trypsin digestion		
peptide	measured mass	expected mass
A $\beta$ (1-5)	636.31	636.29
A $\beta$ (6-16)	1335.60	1335.59
A $\beta$ (6-16)PEG	1934.98	1934.94
A $\beta$ (1-16)	1953.89	1953.87
PEG	617.39	617.36
A $\beta$ (1-16)PEG	2552.2	2552.9
elastase digestion		
peptide	measured mass	expected mass
A $\beta$ (1-12)	1423.65	1423.60
A $\beta$ (13-16)PEG	1147.60	1147.63
A $\beta$ (1-16)PEG	2552.2	2552.9

<sup>a</sup> Measured mass column has been obtained by deconvoluting the experimental multicharged peaks.

Cu-A $\beta$ (1-6) system for which a NH<sub>2</sub>, N<sup>-</sup>, N<sub>im</sub> binding mode was hypothesized.<sup>26</sup> This means that the zinc(II) shifts copper(II) from the multihistidine to the (NH<sub>2</sub>,N<sup>-</sup>,N<sub>im</sub>) binding mode in which the His6 is mainly involved in copper(II) coordination. At the same time, histidyl residues in positions 13 and 14 bind the zinc(II) (Figure 8B).

**Copper(II) and Zinc(II) Modulate the Proteolysis of A $\beta$ (1-16)PEG.** Both copper(II) and zinc(II) complexes with A $\beta$ (1-16)PEG were also studied by means of limited proteolysis carried out at various metal to peptide ratios. Such a technique is particularly effective at characterizing native protein structure<sup>43</sup> as well as partially folded intermediates and flexible sites within proteins.<sup>44</sup> In fact, cleavage of peptide bonds by a protease occurs at exposed or disordered regions of the polypeptide backbone.<sup>45</sup> By contrast, buried and/or structured portions of protein are protected from proteolysis.<sup>46</sup> Limited proteolysis of both uncomplexed and complexed A $\beta$ (1-16)PEG were thus carried out in order to evaluate an eventual metal-induced structuring of the peptide, which is in turn related to the preferred binding site of the different metal ions within the primary sequence of the polypeptide. The experiments were performed using two different proteases, trypsin and elastase, with the aim of obtaining information on different cleavage sites and detecting the presence of zinc(II) or copper(II) at their preferred binding sites.

According to the potentiometric and spectroscopic results indicating the number of coordinated zinc(II) or copper(II) ions per A $\beta$ (1-16)PEG peptide molecule, limited proteolysis experiments were carried out at different metal ion to peptide ratios, ranging from 1:1 to 4:1 for copper(II) and from 1:1 to 3:1 for zinc(II). Peptide fragments generated by the proteolytic action of each enzyme were separated by reversed-phase HPLC and identified by ESI-MS. This allowed the identification of the cleavage sites to be obtained.

In the case of trypsin digestion, two hydrolysis sites can be identified at Arg5 and Lys16, even though the PEG conjugation at the C-terminus decreases the hydrolysis rate at Lys16. Three peptide fragments are therefore produced after trypsin digestion of A $\beta$ (1-16)PEG, namely, A $\beta$ (1-5), A $\beta$ (6-16), and A $\beta$ (6-16)PEG (Table 3). In the absence of metal ions, the

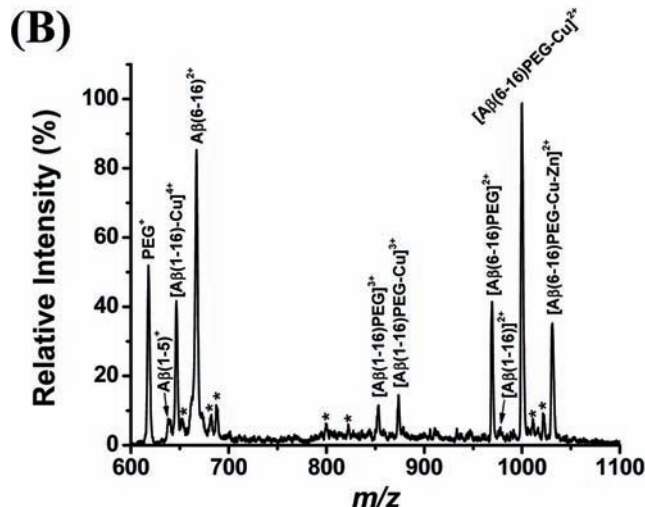
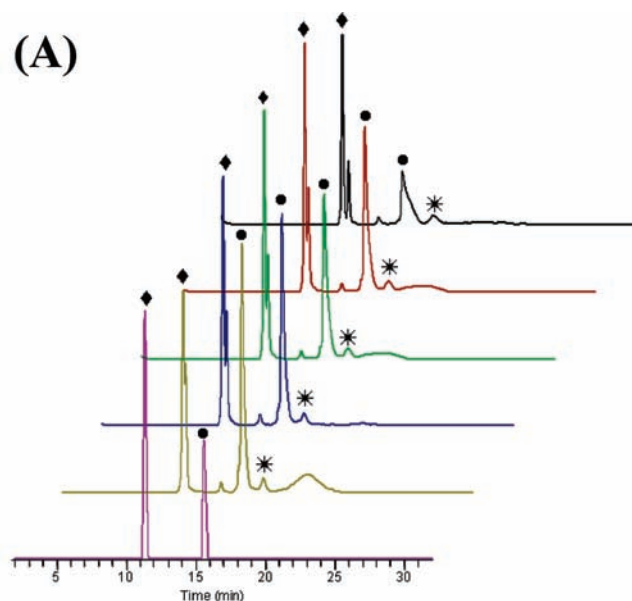


**Figure 9.** (A) HPLC profiles of A $\beta$ (1-16)PEG digested with trypsin in the absence (violet) and in the presence of 1 equiv (yellow), 2 equiv (blue), 3 equiv (green), 4 equiv (red), and 10 equiv (black) of copper(II) [(♦) A $\beta$ (1-5)+A $\beta$ (6-16), (●) A $\beta$ (6-16)PEG, (\*) A $\beta$ (1-16)PEG]. Identical results were obtained if zinc(II) was also present in solution at a copper/zinc ratio of 1:1. (B) Representative mass spectrum obtained for A $\beta$ (1-16)PEG digested with trypsin in the presence of both copper(II) and zinc(II) ions. Impurities and/or sodiated peaks are indicated with an asterisk. Discussion is in the text.

hydrolysis of the Arg5-His6 peptide bond is essentially accomplished after 30 min. Nearly identical results were obtained in the presence of increasing amounts of zinc(II) ions (data not shown). This indicates that this metal ion does not alter the proteolytic accessibility of the N-terminal region of A $\beta$ (1-16)PEG, which remains flexible even in the presence of an excess of zinc(II). By contrast, in the case of copper(II), the presence of intact A $\beta$ (1-16)PEG, detected at Rt = ~17 min in the HPLC profiles (Figure 9A), suggests that 30 min is not sufficient to degrade the copper(II) complexes of A $\beta$ (1-16)PEG. This means that the cleavage of the Arg5-His6 peptide bond is slower in the presence of copper(II) than in the absence of this metal ion. As we checked that copper(II) had no effect on the catalytic rate of trypsin



by running a control experiment on a standard substrate, the slower cleavage must be due to its decreased accessibility caused by copper(II)-induced bending of the region 1–6 of  $A\beta$ -(1–16)PEG. In addition, these results confirm that copper(II) is preferentially located within this amino acid region, whereas zinc(II) resides quite far from this site.

The same experiments were also performed on  $A\beta$ (1–16)PEG in the presence of an equimolar amount of copper(II) and zinc(II), and the results were identical to those obtained in the case of copper(II) alone (see Figure 9B), confirming that zinc coordination does not modify the conformation of binary copper(II) complexes, in agreement with the results obtained by CD. In Figure 9B, a representative mass spectrum obtained for the trypsin digestion (30 min) of  $A\beta$ (1–16)PEG is reported. In this case, both copper(II) and zinc(II) were added, and the proteolysis of  $A\beta$ -(1–16)PEG is not complete (the molecular peak of the peptide as well as the metal–peptide complex is still detected). It is important to highlight that the ternary  $Cu^{2+}-Zn^{2+}-A\beta$ (6–16)PEG complex is also detected in this case (zoom scan mode was applied to distinguish this complex from the  $Cu_2^{2+}-A\beta$ (6–16)PEG, data not shown), proving once again that, in the ternary complex, the binding of zinc(II) occurs in this portion of the peptide, in accordance with the spectroscopic results.

Leukocyte elastase has a preferential cleavage for the carboxyl side of valine residues. Two peptide fragments, e.g.,  $A\beta$ (1–12) and  $A\beta$ (13–16)PEG (see Table 3), are generated after elastase digestion of  $A\beta$ (1–16)PEG, which is totally degraded in 75 min. In the presence of copper(II) or zinc(II), the rate of the hydrolysis decreases, as demonstrated by the detection of intact  $A\beta$ (1–16)PEG in the HPLC profiles after 75 min of reaction (data not shown). Therefore, both metal ions should be coordinated to amino acid residues close to the putative site of cleavage, which is the Val12–His13 peptide bond. Interestingly, the HPLC profiles show that the concentration of intact  $A\beta$ (1–16)PEG increases as a function of copper(II) or zinc(II) concentration. This is in agreement with the potentiometric results, indicating that more than one metal ion can be coordinated in this peptide region.

## CONCLUSIONS

A huge number of studies have been performed to determine the affinities and to clarify the major binding sites and aggregation forms of the d block metal ions with  $A\beta$  peptides. Different coordination environments have been proposed for the different  $A\beta$  complexes on the basis of several spectroscopic techniques including NMR, Raman spectroscopy, circular dichroism, and electrospray-ionization mass spectrometry (ESI-MS).<sup>47–49</sup> However, in past works, only the estimated  $K_d$ , the dissociation constant, could be obtained. Although useful, this can only give an estimation of the various components at different pH's and metal to ligand ratios, without giving further information on the binding details. On the contrary, in this work, by using the  $\beta$  approach (the “overall” complex-formation constant), the affinity of the different metal complex species and their coordination environments could be obtained.

Moreover, the previous investigations have been focused on the interactions with “single” metal ions, while it is difficult to find similar studies involving “multiple” metal ion interactions with  $A\beta$ , though in the brains of AD patients the different metals coexist at altered concentrations. Of course, complex formation is always a competition, but in the case of the copper(II)–zinc(II)– $A\beta$  complex, the two different metal ions have different

affinities toward the independent binding sites of the peptides. Indeed, we have found that the addition of zinc(II) does not simply liberate copper(II) but modifies the distribution of the metal ions among the available binding sites.

The completely different metal ion affinity of the N-terminus and the His13–His14 sites of the  $A\beta$ (1–16)PEG provides an idealized set of donor atoms for the formation of mixed metal copper(II)–zinc(II) species. Our results indicate that, when copper(II) to zinc(II) ratios are low,  $A\beta$ (1–16)PEG can simultaneously bind copper(II) and zinc(II). The  $Zn^{2+}$  is accommodated by shifting the  $Cu^{2+}$  to binding modes that minimize the interactions of histidines with  $Cu^{2+}$ . However, the copper(II) is not displaced from the N-terminal group, which is its preferred coordinating site. Together, these findings complete the picture of the binding modes of these metal ions, previously reported for their simple complex species. We have found that increasing the metal to peptide ratio produces the formation of different isomeric forms of copper(II)– $A\beta$  species due to the stepwise independent anchoring ability of the different histidine residues that drive the deprotonation of the amide nitrogens with consequent conformational changes of the peptide.<sup>26</sup> The formation of deprotonated species is likely to be responsible for the unfibrillar aggregates.

We have found that the same independent metal binding is maintained even when the copper(II) is partly substituted by zinc(II) and that the complex formation process of  $A\beta$  is strongly dependent on the concentrations of both the peptide and the metal ions. This has considerable impact on the speciation process. In fact, our data indicate that the stoichiometry of the main complexes, around physiological pH, changes as a function of the metal to peptide ratio considered. Taking into account that copper(II), zinc(II), and  $A\beta$  concentrations in the brain and CNS vary from region to region, the major complex species formed in different districts of the brain will be different. This may also affect the  $A\beta$  toxicity and aggregation pathways, which are both dependent on the metal ions binding. Zinc(II) in the brain reaches levels up to 300  $\mu$ M in the synaptic cleft of the glutaminergic neurons.<sup>50</sup> This concentration value is higher than that found for copper(II) in the same district (30  $\mu$ M), and for this reason, we explored high zinc(II) to copper(II) ratios to mimic the brain levels of the two metal ions. Our results show that  $Zn^{2+}$  is not able to completely substitute  $Cu^{2+}$ , and more interesting, copper(II) is shifted from the binding to the two His residues, His13 and His14, a condition invoked by other authors to explain the redox activity of copper– $A\beta$  complexes.<sup>51</sup>

The formation of ternary metal complexes, therefore, may justify the protective role of zinc in comparison with copper.

## AUTHOR INFORMATION

### Corresponding Author

\*Tel: +39(0)957385070 (E.R.). Fax: +39(0)95337678 (E.R.), (+) 36-52-489667 (I.S.). E-mail: erizzarelli@unict.it (E.R.), sovago@delfin.unideb.hu (I.S.).

## ACKNOWLEDGMENT

Support by MIUR, FIRB-RBPR05JH2P and FIRB-RBNE-08HWLZ, the MTA (Hungary)-CNR(ITALY) bilateral program, OTKA 77586, and TAMOP 4.2.1/B-09/1/KONV-2010-0007 project (Hungary) are gratefully acknowledged.



## REFERENCES

- (1) Hardy, J.; Selkoe, D. J. *Science* **2002**, *297*, 353–356.
- (2) Crouch, P. J.; Harding, S.-M. E.; White, A. R.; Camakaris, J.; Bush, A. I.; Masters, C. L. *Int. J. Biochem. Cell Biol.* **2008**, *40*, 181–198.
- (3) Selkoe, D. J. *Physiol. Rev.* **2001**, *81*, 741–766.
- (4) Bush, A. I.; Pettingell, W. H.; Multhaup, G.; Paradis, M. D.; Vonsattel, J. P.; Gusella, J. F.; Beyreuther, K.; Masters, C. L.; Tanzi, R. E. *Science* **1994**, *265*, 1464–1467.
- (5) Stoltenberg, M.; Bush, A. I.; Bach, G.; Smidt, K.; Larsen, A.; Rungby, J.; Lund, S.; Doering, P.; Danscher, G. *Neuroscience* **2007**, *150*, 357–369.
- (6) Shearer, J.; Szalai, V. A. *J. Am. Chem. Soc.* **2008**, *130*, 17826–17835.
- (7) Atwood, C. S.; Moir, R. D.; Huang, X.; Scarpa, R. C.; Bacarra, N. M.; Romano, D. M.; Hartshorn, M. A.; Tanzi, R. E.; Bush, A. I. *J. Biol. Chem.* **1998**, *273*, 12817–12826.
- (8) Dyrks, T.; Dyrks, E.; Hartmann, T.; Masters, C.; Beyreuther, K. *J. Biol. Chem.* **1992**, *267*, 18210–18217.
- (9) Ali, F. E.; Separovic, F.; Barrow, C. J.; Yao, S. G.; Barnham, K. *Int. J. Pept. Res. Ther.* **2006**, *12*, 153–164.
- (10) Lim, K. H.; Kim, Y. K.; Chang, Y. T. *Biochemistry* **2007**, *46*, 13523–13532.
- (11) Mantyh, P. W.; Ghilardi, J. R.; Rogers, S.; DeMaster, E.; Allen, C. J.; Stimson, E. R.; Maggio, J. E. *J. Neurochem.* **1993**, *61*, 1171–1174.
- (12) Miura, T.; Suzuki, K.; Kohata, N.; Takeuchi, H. *Biochemistry* **2000**, *39*, 7024–7031.
- (13) Raman, B.; Ban, T.; Yamaguchi, K. I.; Sakai, M.; Kawai, T.; Naiki, H.; Goto, Y. *J. Biol. Chem.* **2005**, *280*, 16157–16162.
- (14) Hou, L. M.; Zagorski, M. G. *J. Am. Chem. Soc.* **2006**, *128*, 9260–9261.
- (15) Zou, J.; Kajita, K.; Sugimoto, N. *Angew. Chem., Int. Ed. Engl.* **2001**, *40*, 2274–2277.
- (16) Yoshiike, Y.; Tanemura, K.; Murayama, O.; Akagi, T.; Murayama, M.; Sato, S.; Sun, X. Y.; Tanaka, N.; Takashima, A. *J. Biol. Chem.* **2001**, *276*, 32293–32299.
- (17) Ryu, J.; Girigoswami, K.; Ha, C.; Ku, S. H.; Park, C. B. *Biochemistry* **2008**, *47*, 5328–5335.
- (18) Lee, J. S.; Ryu, J.; Park, C. B. *Anal. Chem.* **2009**, *81*, 2751–2759.
- (19) Jun, S.; Gillespie, J. R.; Shin, B.; Saxena, S. *Biochemistry* **2009**, *48*, 10724–10732.
- (20) Dong, J.; Shokes, J. E.; Scott, R. A.; Lynn, D. G. *J. Am. Chem. Soc.* **2006**, *128*, 3540–3542.
- (21) Karr, J. W.; Kaupp, L. J.; Szalai, V. A. *J. Am. Chem. Soc.* **2004**, *126*, 13534–13538.
- (22) Dong, J.; Canfield, J. M.; Mehta, A. K.; Shokes, J. E.; Tian, B.; Childers, W. S.; Simmons, J. A.; Mao, Z.; Scott, R. A.; Warncke, K.; Lynn, D. G. *Proc. Nat. Acad. Sci. U. S. A.* **2007**, *104*, 13313–13318.
- (23) Miller, Y.; Ma, B.; Nussinov, R. *Proc. Natl. Acad. Sci. U. S. A.* **2010**, *107*, 9490–9495.
- (24) Minicozzi, V.; Stellato, F.; Comai, M.; Dalla Serra, M.; Potrich, C.; Meyer-Klaucke, W.; Morante, S. *J. Biol. Chem.* **2008**, *283*, 10784–10792.
- (25) Damante, C. A.; Ösz, K.; Nagy, Z.; Pappalardo, G.; Grasso, G.; Impellizzeri, G.; Rizzarelli, E.; Sóvágó, I. *Inorg. Chem.* **2009**, *48*, 10405–10415.
- (26) Damante, C. A.; Ösz, K.; Nagy, Z.; Pappalardo, G.; Grasso, G.; Impellizzeri, G.; Rizzarelli, E.; Sóvágó, I. *Inorg. Chem.* **2008**, *47*, 9669–9683.
- (27) Brown, D. R.; Kozłowski, H. *Dalton Trans.* **2004**, 1907–1917.
- (28) Gaggelli, E.; Kozłowski, K.; Valensin, D.; Valensin, G. *Chem. Rev.* **2006**, *106*, 1995–2044.
- (29) Faller, P.; Hureau, C. *Dalton Trans.* **2009**, 1080–1094.
- (30) Hatcher, L. Q.; Hong, L.; Bush, W. D.; Carducci, T.; Simon, J. D. *J. Phys. Chem. B* **2008**, *112*, 8160–8164.
- (31) Sarell, C. J.; Syme, C. D.; Rigby, S. E. J.; Viles, J. H. *Biochemistry* **2009**, *48*, 4388–4402.
- (32) Atwood, C. S.; Moir, R. D.; Huang, X.; Scarpa, R. C.; Bacarra, N. M.; Romano, D. M.; Harthorn, M. A.; Tanzi, R. E.; Bush, A. I. *J. Biol. Chem.* **1998**, *273*, 12817–12826.
- (33) Atwood, C. S.; Scarpa, R. C.; Huang, X.; Moir, R. D.; Jones, W. D.; Fairlie, D. P.; Tanzi, R. E.; Bush, A. I. *J. Neurochem.* **2000**, *75*, 1219–1233.
- (34) Guilloreau, L.; Damian, L.; Coppel, Y.; Mazarguil, H.; Winterhalter, M.; Faller, P. *J. Biol. Inorg. Chem.* **2006**, *11*, 1024–1038.
- (35) Clements, A.; Allsop, D.; Walsh, D. M.; Williams, C. H. *J. Neurochem.* **1996**, *66*, 740–747.
- (36) Drochioiu, G.; Manea, M.; Dragusanu, M.; Murariu, M.; Dragan, E. S.; Petre, B. A.; Mezo, G.; Przybylski, M. *Biophys. Chem.* **2009**, *144*, 9–20.
- (37) Jozsa, E.; Ösz, K.; Kallay, C.; De Bona, P.; Damante, C. A.; Pappalardo, G.; Rizzarelli, E.; Sóvágó, I. *Dalton Trans.* **2010**, 39, 7046–7053.
- (38) Zékány, L.; Nagypál, I. In *Computational Methods for the Determination of Formation Constants*; Leggett, D. J., Ed.; Plenum Press: New York, 1985; pp 291–355.
- (39) Gans, P.; Sabatini, A.; Vacca, A. *J. Chem. Soc., Dalton Trans.* **1985**, 1195–1200.
- (40) Gans, P.; Sabatini, A.; Vacca, A. *Talanta* **1996**, *43*, 1739–1753.
- (41) Tsangaris, J. M.; Chang, J. W.; Martin, R. B. *J. Am. Chem. Soc.* **1969**, *91*, 726–731.
- (42) Fawcett, T. G.; Bernarducci, E. E.; Krough-Jespersen, K.; Schugar, H. J. *J. Am. Chem. Soc.* **1980**, *102*, 2598–2604.
- (43) Neurath, H. In *Protein Folding*; Jaenicke, R., Ed.; Elsevier, Amsterdam, 1980, 501–523.
- (44) Fontana, A.; de Laureto, P. P.; De Filippis, V.; Scaramella, E.; Zambonin, M. *Fold. Des.* **1997**, *2*, R17–R26.
- (45) Hubbard, S. J. *Biochim. Biophys. Acta* **1998**, *1382*, 191–206.
- (46) Zhao, Y.; Chait, B. T. *Anal. Chem.* **1994**, *66*, 3723–3726.
- (47) Mekmouche, Y.; Coppel, Y.; Hochgrafe, K.; Guilloreau, L.; Talmard, C.; Mazarguil, H.; Faller, P. *ChemBioChem* **2005**, *6*, 1663–1671.
- (48) Syme, C. D.; Viles, J. H. *Biochim. Biophys. Acta* **2006**, *1764*, 246–256.
- (49) Danielsson, J.; Pierattelli, R.; Banci, L.; Graslund, A. *FEBS J.* **2007**, *274*, 46–59.
- (50) Que, E. L.; Domaille, D. W.; Chang, C. J. *Chem. Rev.* **2008**, *108*, 1517–1549.
- (51) Himes, R. A.; Park, G. Y.; Siluvai, G. S.; Blackburn, N. J.; Karlin, D. K. *Angew. Chem., Int. Ed.* **2008**, *47*, 9084–9087.